^{129}Xe NMR Study of Adsorption and Dynamics of Xenon in AgA Zeolite†

Igor L. Moudrakovski,* Christopher I. Ratcliffe, and John A. Ripmeester

Contribution from the Steacie Institute for Molecular Sciences, National Research Council, Ottawa, Ontario, Canada K1A 0R6

Received October 29, 1997

Abstract: The adsorption of xenon in AgA zeolite has been studied by ^{129}Xe NMR spectroscopy, yielding information on the silver distribution, Xe cluster size and distribution, and xenon exchange dynamics. The exchange of xenon is slow between the α-cages of AgA treated in a vacuum at 380 or 410 K (yellow AgA), and separate lines appear in the ^{129}Xe NMR spectra for cages containing different xenon populations. Up to 10 different Xe_n clusters with n between 1 and 8 can be distinguished; the Xe_7 and Xe_8 clusters appear to be present in two different states $Xe_7' + Xe_7''$ and $Xe_8' + Xe_8''$, reflecting cage differences apparent only at high xenon loading. The population distribution, studied over a broad range of xenon loadings, cannot be described in terms of the simple hypergeometric distribution except at loading levels below $n = 4$. The Xe_n cluster lines for "yellow" AgA zeolite are all shifted uniformly to low field relative to the clusters in NaA zeolite, a feature which currently has no firm explanation. Because large xenon clusters up to Xe_8 can reside in the α cage, size constraints lead one to conclude that any charged silver clusters must be located inside the sodalite (β) cages. The uptake and redistribution of xenon in the zeolite is relatively slow (hours to weeks). The slow passage of xenon atoms through the 8-rings can be attributed to the presence of a hydrated silver ion at the aperture. This blocking effect disappears for samples annealed at higher temperatures to give "orange" AgA. Xenon exchange dynamics between the cages has been studied in detail by applying 2D-EXSY NMR methods. All of the exchange constants can be obtained directly from the analysis of the 2D-NMR data, and from variable-temperature 2D EXSY experiments. The activation energy of xenon transfer between the different cages can be estimated to be 45 ± 10 kJ/mol, significantly lower than for NaA zeolite. Cage-to-cage exchange rate constants increase with the degree of loading above ca. $n = 4$, reflecting decreased sorption energies at higher loading.

Introduction

Since its first applications to the study of microporous solids,[1,2] ^{129}Xe NMR has become a very popular technique for the study of zeolites and other porous materials. In many respects xenon provides a very convenient probe for the NMR study of systems with void spaces. It is chemically inert, monatomic, has a convenient size, and possesses suitable NMR properties. There are several reviews on the application of xenon NMR to microporous materials.[3−7]

The technique is able to provide valuable information on the structure of the adsorbent, the distribution of xenon within the pore structure, the occupancies of different sites, and the rates of transfer of xenon between the different regions. In principle, data from ^{129}Xe NMR studies can be further used for the modeling of adsorption properties of other molecules. Despite numerous empirical observations, however, the predictive capabilities of the method are still limited by a lack of a comprehensive theory for Xe NMR chemical shifts in zeolites, though significant steps are being taken in this direction.[8,9,13−15] A serious limitation is that for most systems the observed signals are averaged by fast exchange, and thus cannot be assigned directly to any particular site or structure. In this regard, studies of systems where the processes of exchange are limited play an important role in obtaining reliable information concerning the relationship between ^{129}Xe NMR parameters and the pore structure.

Recent studies of distribution functions and the dynamics of xenon in NaA and KA zeolites, systems with very slow exchange of xenon between the zeolite cages, have demonstrated the great potential of ^{129}Xe NMR as a tool for probing the

† Published as NRCC No. 40864.

* To whom all correspondence should be addressed. Phone: (613) 993 5638. FAX: (613) 998 7833. E-mail: igorm@ned1.sims.nrc.ca.

(1) Ito, T.; Fraissard, J. *J. Chem. Phys*. **1982**, *76*, 5225.
(2) Ripmeester, J. A. *J. Am. Chem. Soc*. **1982**, *104*, 289.
(3) Raftery, D.; Chmelka, B. F. *NMR Basic Princ. Prog*. **1994**, *30*, 111.
(4) Dybowski, C.; Bansal, N.; Duncan, N. T. *Annu. Rev. Phys. Chem*. **1991**, *42*, 433.
(5) Fraissard, J.; Ito, T. *Zeolites* **1988**, *8*, 350.
(6) Barrie, P. J.; Klinowski, J. *Prog. NMR Spectrosc*. **1992**, *24*, 91.
(7) Springuel-Huet, M.-A.; Bonardet, J.-L.; Fraissard, J. *Appl. Magn. Reson*. **1995**, *8*, 427.
(8) Jameson, C. J.; Jameson, K. A.; Baello, B. I.; Lim, H.-M. *J. Chem. Phys*. **1994**, *100*, 5965.
(9) Jameson, C. J.; Jameson, K. A.; Lim, H.-M.; Baello, B. I. *J. Chem. Phys*. **1994**, *100*, 5977.
(10) Jameson, C. J.; Jameson, K. A.; Gerald, R., II; de Dios, A. C. *J. Chem. Phys*. **1992**, *96*, 1676.
(11) Jameson, C. J.; Jameson, K. A.; Gerald, R., II; de Dios, A. C. *J. Chem. Phys*. **1992**, *96*, 1690.
(12) Jameson, A. K.; Jameson, C. J.; de Dios, A. C.; Oldfield, E.; Gerald, R. E., II; Turner, G. L. *Solid State Nucl. Magn. Reson*. **1995**, *4*, 1.
(13) Jameson, A. K.; Jameson, C. J.; Gerald, R. E., II *J. Chem. Phys*. **1994**, *101*, 1775.
(14) Jameson, C. J.; Jameson, A. K.; Gerald, R. E., II; Lim, H.-M. *J. Chem. Phys*. **1995**, *103*, 8811.
(15) Jameson, C. J.; Jameson, A. K.; Lim, H.-M. *J. Chem. Phys*. **1996**, *104*, 1709.

S0002-7863(97)03748-7 CCC: $15.00 Published 1998 by the American Chemical Society
Published on Web 03/20/1998

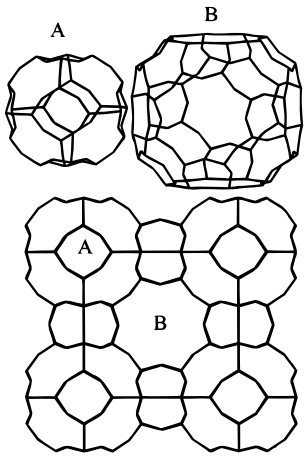

Figure 1. Structure of zeolite A. Small (A) and large (B) cages of the zeolite are shown.

fundamentals of the adsorption processes.[8−17] Significant insight into the nature of xenon chemical shifts in zeolites has been achieved with the aid of Grand Canonical Monte Carlo (GCMC) simulations.[8,9,13−15] GCMC calculations of Xe in NaA and KA zeolites have provided a quantitative explanation of ^{129}Xe chemical shifts, and a basis for understanding average ^{129}Xe NMR chemical shifts in other microporous solids, where xenon is in fast exchange between many sites.

In this work we present the results of a ^{129}Xe NMR study of xenon in AgA zeolite—a system where exchange between the cages is also significantly constrained. Completely exchanged zeolite AgA has a cubic lattice with $a = 24.5$ Å, and a unit cell content before calcination of $\{Ag_{12}[Al_{12}Si_{12}O_{48}](20-25)H_2O\}_8$. The pore system in A zeolite is formed by large α-cages connected through eight-membered Si−O−Si rings with an opening of about 4.1 × 4.1 Å, taking into account the O atoms' van der Waals radii (Figure 1). For many years, AgA zeolite (along with AgX and AgY) was a popular system in studies concerning the structure, transformation, and reactive properties of small metal clusters (reviewed in ref 18). Sensitivity to light and reversible oxidation/reduction properties make silver-exchanged zeolites possible candidates for novel optical and electronic materials. There is also a substantial interest in these materials because of the pronounced catalytic activity of the silver. When Ag A zeolite is dehydrated by heating under vacuum, partial reduction of Ag^+ takes place thus forming charged Ag clusters inside the zeolite cages. The extent of the Ag^+ reduction is a function of temperature. Temperatures of ∼370−420 K produce the "yellow form" of the material, whereas calcination at 670−700 K results in an "orange form". The yellow color has been attributed to the formation of Ag_3^{2+} clusters, and the orange color is explained by the formation of larger size clusters.[18,19] Despite considerable effort, the composition and location of the clusters are still in question. Generally it is believed that the silver clusters forming at high temperature are located inside the β-cages.[18]

Similar to zeolite NaA, the exchange of xenon atoms between the α-cages in AgA is slow on the NMR time scale, and Xe adsorption in AgA treated below 470 K produces a ^{129}Xe NMR spectrum with separate lines for cages with different xenon populations.[20,21] Such a system is interesting from several points of view. First, the equilibrium distributions (and chemical shifts) of xenon atoms trapped inside the large cages provide a benchmark for comparison of the adsorption and diffusion properties predicted by molecular dynamics simulations and chemical shift calculations.[8,9] The location and the structure of the silver cations and the effect of residual water on diffusion properties are also of interest. Since the framework is basically the same as in NaA, we may study the effects of the location and the nature of the cations on the Xe adsorption properties.

While the AgA system is more complex than NaA, many processes are expected to be similar, and can be understood by comparing the data for both systems. Xenon in NaA has been the subject of extensive studies in different laboratories,[8−10,13,16,17] which provides us with a solid base for understanding our experimental data. In this work special attention will be paid to (i) distribution of xenon in the zeolite cages, (ii) localization of charged silver clusters and molecules of residual water in the zeolite's structure, and (iii) xenon dynamics in AgA zeolite. Very recently, calculations of chemical shifts and cage size distributions have been performed on the Xe/AgA system and compared with some of our experimental data.[22] We will refer to this work at appropriate points in the text.

Experimental Section

Sample Preparation. Zeolite AgA was prepared by ion exchange of Linde A zeolite in a 1 M water solution of $AgNO_3$. The quantity of solution was sufficient to provide a 3-fold excess of Ag^+ cations as required for 100% exchange. The NaA zeolite was stirred with this solution in darkness for 24 h, then filtered, washed in distilled water, and dried in air at room temperature. The extent of exchange was monitored by ^{23}Na MAS NMR (residual sodium cations <2% of the initial quantity).

The thermal treatment of the AgA zeolites and the adsorption of xenon were carried out on a standard vacuum line in 30−40 mm long glass tubes (10 mm o.d.). Sample weights typically were about 1 g. To limit the dead volume, space-filling pieces of glass rod were inserted into the tubes, thus confining the sample to one end. The samples were evacuated while heating at approximately 1 K/min up to either 380 or 410 K and were then left for a further 20−25 h at these temperatures. After cooling, a known quantity of xenon gas was condensed onto the samples at 77 K, and the tubes were sealed. Sealed samples for magic angle spinning experiments were prepared in the same way, but with 5 mm o.d. NMR tubes (35 mm long). A few samples were also prepared with enriched ^{129}Xe (ISOTEC Inc.), 79.6% compared with the natural abundance value of 26.44%.

After dehydration in a vacuum at 380 or 410 K the samples had a bright yellow color. Several samples dehydrated at 670 K developed a brick-orange color. We also prepared several samples of xenon in zeolite NaA dehydrated at 670 K. The following notation will be used for the samples names: AgA-380-4.3 means a sample of AgA zeolite dehydrated at 380 K with an average Xe loading ($\langle Xe \rangle$) of 4.3 atoms/α-cage.

The approach to the Xe equilibrium distribution was monitored by observing the changes in ^{129}Xe 1D NMR spectra. Equilibration of the samples (except AgA-670) is very slow, requiring several weeks to complete at room temperature. The process can be accelerated as for NaA by keeping the samples at elevated temperature for several hours[10] (in boiling water in this case), and then slowly reducing the temperature to ambient. Redistribution of xenon between the cages in a sample which has already equilibrated at a different temperature does not take

(16) Chmelka, B. F.; Raftery, D.; McCornick, A. V.; Menorval, L. C.; Levine, R. D.; Pines, A. *Phys. Rev. Lett*. **1991**, *66*, 580.
(17) Larsen, R. G.; Shore, J.; Shmidt-Rohr, K.; Emsley, L.; Long, H.; Pines, A.; Janicke, M.; Chmelka, B. F. *Chem. Phys. Lett*. **1993**, *214*, 220.
(18) Sun, T.; Seff, K. *Chem. Rev.* **1994**, *94*, 857.
(19) Gellens, L. R.; Mortier, W. J.; Uytterhoeven, J. B. *Zeolites* **1981**, *1*, 11. (b) Gellens, L. R.; Mortier, W. J.; Schoonheydt; Uytterhoeven, J. B. *J. Phys. Chem*. **1981**, *85*, 2783.
(20) Ripmeester, J. A.; Ratcliffe, C. I. *Proceedings of the 9th International Zeolite Conference*: Montreal, 1992; p 572.
(21) Moudrakovski, I. L.; Ratcliffe, C. I.; Ripmeester, J. A. In *Zeolites: A refined tool for designing Catalytic Sites*; Bonneviot, L., Kaliaguine, S., Eds.; Elsevier Science: Amsterdam, 1995; pp 243−250.
(22) Jameson, C. J.; Lim, H.-M. Private communication.

very long; however, care still has to be taken to provide enough time at the new temperature of equilibration. Redistribution of xenon between the cages was verified by monitoring 1D spectra. Thus, for the variable-temperature experiments it was necessary for the samples to be kept at the temperature of the experiment for as long as 2−4 h before obtaining spectra.

For all samples prepared in this manner, the presence of excess xenon in the gas phase must be taken into account when estimating the Xe loading inside the zeolite. The correction for our samples was done according to the procedure described in detail by Jameson et al.[10] Since the tubes were calibrated only volumetrically, the precision in determining the void spaces in our samples was less than that in ref 10; however, in all cases it was better than 10%.

NMR Measurements. All ^{129}Xe NMR experiments were carried out on a Bruker AMX300 spectrometer at 83.013 MHz, using a homemade probe with a solenoid coil for static experiments and a Chemagnetics 7.5-mm MAS probe for MAS experiments. The 90-degree pulse was 4−5 μs for both probes, and relaxation delays were in the range of 60−100 s. Usually 16 to 128 scans gave signal-to-noise ratios better than 30. All ^{129}Xe chemical shifts are referred to that of Xe gas at zero pressure (0 ppm).

1D spectra were acquired with the usual one-pulse phase-cycled sequence. Relaxation times T_1 were measured with use of the inversion recovery $\pi-\tau-\pi/2$ method. Cross-polarization spectra were obtained with a proton radio frequency field strength $\omega_{1H} = 60$ kHz and relaxation delay of 4 s. The cross-polarization time constants, T_{CPXe-H}, and the proton spin−lattice relaxation times in the rotating frame, $T_{1\rho}$, were found from analysis of the variable contact time experiments. 2D-Exchange NMR spectra were acquired with a standard 3-pulse sequence with use of TPPI.[23] Mixing times were varied in the range 10 ms to 2 s. Usually 64 and 256 points were acquired in the t_1 and t_2 dimensions. From 16 to 64 scans were made per t_1 point depending on the sample. Before Fourier transformation the t_1-dimension was zero filled to 256 points, 100 Hz Gaussian broadening was applied in the F2 dimension, and sinusoidal multiplication was applied in the F1 dimension. Integration of the 2D-spectra was performed with standard spectrometer software. For calculation of magnetization exchange constants from the 2D spectra we developed a PC program, based on the approach described in ref 24.

Results and Discussion

The ^{129}Xe NMR spectra of samples with different loadings of xenon in zeolite AgA-380 and AgA-410 are shown in Figures 2 and 3. The spectra of xenon in AgA-670 and NaA are also shown for comparison. The sharp line near 0 ppm is assigned to Xe gas in the space between crystallites. Note that this line is observed for AgA zeolite only at very high loadings ($\langle$Xe$\rangle$ > 5 atom/cage), whereas in NaA the gas line is present even at relatively low loadings. This indicates easier access to the cages in AgA zeolite than in NaA. All the other lines in the spectra, at lower field, can be assigned to xenon atoms trapped inside the α-cages with different populations of xenon atoms with the highest field line corresponding to 1 Xe/α-cage. The progression of lines to lower field then corresponds to cages with 2 up to 8 Xe. The observation of separate lines in the spectra indicates that the interchange of xenon atoms between different cages is slow on the NMR time scale (less than 1500−2000 s^{-1} based on the separation of the lines in hertz).

The shape of lines 7 and 8 in the static spectra (Figure 4, top) suggests the presence of axial chemical shift anisotropy; however, MAS experiments show that this is not the case; each of these lines actually is a superposition of two signals (Figure 4, middle). Although we did not observe such additional lines

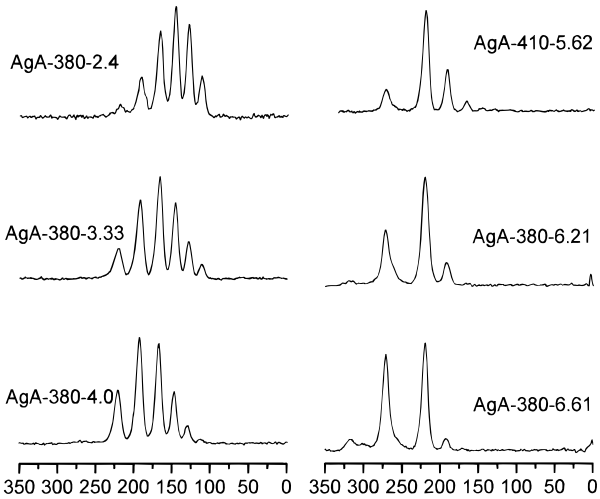

Figure 2. ^{129}Xe NMR spectra of Xe in AgA-380 and AgA-410 zeolites with different $\langle n \rangle$.

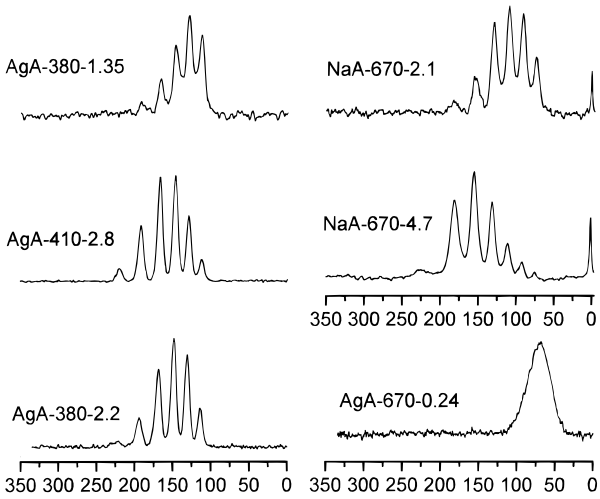

Figure 3. Representative ^{129}Xe NMR spectra of Xe in AgA-380 with different $\langle n \rangle$, NaA-670 and AgA-670.

for xenon in NaA samples, Jameson et al.[12] report similar behavior in samples of NaA of different origin. The effect can be explained in terms of cages with different structural details. Jameson et al. also found that the Ca^{2+} content of NaA affects this behavior. In fact NaA is known to undergo a phase transition at about 335 K. Another plausible explanation, which we favor in the present case, is that clusters of 7 or 8 Xe force local structural changes in some of the α-cages. Perhaps, depending on the Xe and Ag content of neighboring cages, the α-cage expands slightly to better accommodate 7 or 8 xenon atoms. A strong indication that this is a local structural change is that bulk changes should cause shifts in all the lines, as observed by Jameson et al.[12] for NaA samples in which high- and low-temperature crystal forms were present.

Unlike AgA-380(410) and NaA-670, such separate lines are not observed for AgA-670. Instead, we observe a broad line, which is apparently a result of relatively fast exchange between the cages, suggesting that the 8-ring windows are no longer blocked. The position of the line, close to 60 ppm, is relatively independent of the loading in the range studied, i.e., $\langle$Xe$\rangle$ between 0.2 and 1.2 atom/cage. We also note that the chemical shift is much smaller than one might expect from a simple exchange averaging for a yellow AgA sample with similar xenon loading.

(23) Ernst, R.; Bodenhausen, G.; Wokaun, A. *Principles of Nuclear Magnetic Resonance in One and Two Dimensions*; Clarendon Press: Oxford, 1992; pp 499 and 528.

(24) Abel, E. W.; Coston, T. P. J.; Orrell, K. G.; Sik, V.; Stephenson, D. *J. Magn. Reson.* **1986**, *70*, 34.

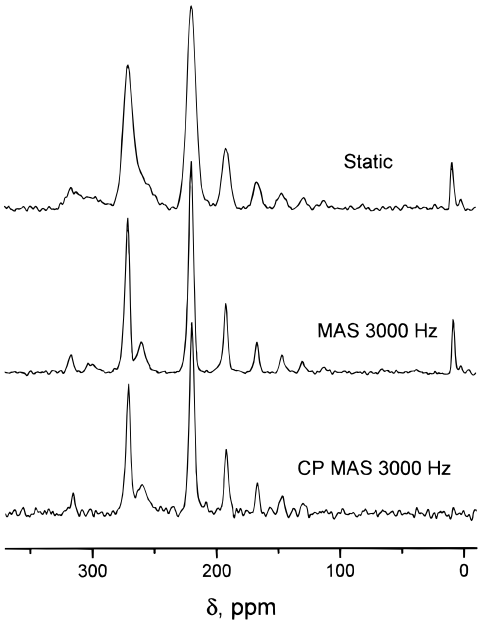

Figure 4. ^{129}Xe MAS and CP MAS NMR spectra of Xe in AgA-380.

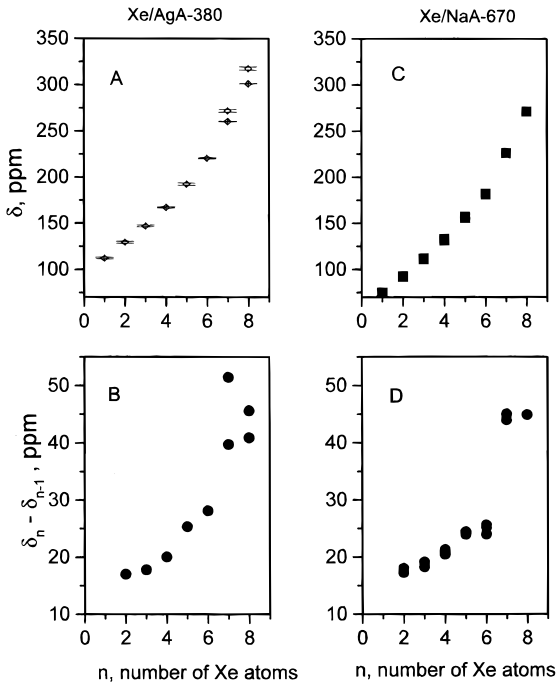

Figure 5. ^{129}Xe Chemical shift of Xe in AgA-380 vs *n* (A) and ΔC.S. vs *n* (B) in comparison with the chemical shifts for Xe_n in NaA-670 (C and D).

Chemical shifts. Figure 5 displays the ^{129}Xe chemical shifts of xenon in the α-cages of zeolite AgA-380 with different populations. Chemical shifts for Xe in NaA-670 are also given for comparison. Our data for AgA resemble closely the data reported previously[10] for NaA. A dependence of the shifts on average loading is not observed. The separation between neighboring peaks for both zeolites is very similar, but for AgA all lines are shifted by about 40 ppm to low field relative to the corresponding lines in NaA. On going from 1 to 6 Xe atoms/cage the separation increment rises slowly from about 17 to 25 ppm, but this number almost doubles for the cages with 7 and 8 Xe atoms. Analogous effects were observed for xenon chemical shifts in NaA,[10] and were quantitatively explained on the basis of GCMC simulations for both NaA[8,9] and AgA.[22]

While the general trends in the chemical shifts of xenon clusters in AgA are the same as for NaA, it is difficult to explain the large downfield shift of the signals in AgA compared with NaA. It is well established, that in silver-exchanged zeolites X and Y after oxidation treatment at elevated temperatures the ^{129}Xe NMR signals are shifted significantly toward *high* field, and shifts extrapolated to zero loading were reported to be as low as −50 ppm.[25] These very unusual high field shifts were explained as being caused by specific interactions of xenon with Ag^+ ions in the SIII positions in the X and Y frameworks.[26,27] It would be natural to expect similar, or even larger (because of the smaller size of the cage, and higher probability of the contact between xenon and Ag^+), chemical shifts of xenon in AgA. Such a high-field shift, however, is not observed in our results for xenon in yellow AgA.

Xenon−xenon interactions would not be expected to be significantly larger inside the α-cages of AgA than in NaA. The cubic lattice constant a_0 for AgA and NaA is almost the same, so the size of the α-cages cannot be significantly different. The presence of residual water molecules inside the cage may be responsible in part for the increased shift.[22] The chemical shifts for xenon clusters in the α-cages of NaA containing coadsorbed water are known to increase somewhat depending on the loading densities of both water and xenon.[28] However, below 4 Xe/cage the effect of water is negligible, even when there are about 3 water molecules in the cage.[28] This is quite different from our observations for AgA.

Jameson et al.[22] have suggested that the low-field shift relative to Xe in NaA may have its origins in the interaction of Xe with a delocalized unpaired electron of an Ag_3^{2+} cluster in the sodalite (*β*) cage via a Fermi contact interaction. However, this does leave the problem that no-one, including ourselves, has been able to find EPR signals in nonirradiated samples.[29] Even the original proponents of the Ag_3^{2+} clusters were unable to confirm its identity by EPR.[19b] Furthermore, the species observed in their X-ray study appeared to be a linear combination of 3 Ag atoms or ions,[19b] whereas EPR observation of Ag_3^{2+} after *γ*-irradiation of yellow AgA[29] showed this species to be triangular as expected from theory. Clearly, the exact description of the cluster still requires more attention. However, we can safely conclude on the basis of the packing constraints for Xe_8 that charged silver clusters are not present in the α-cages of yellow AgA zeolite. The 40 ppm shift discrepancy between Xe in NaA and AgA zeolites thus remains unexplained.

The situation is more complicated for the orange AgA-670 sample: at low loading the chemical shift is ∼60 ppm and nearly independent of loading. As we have noted earlier, the chemical shift is now shifted toward high field when compared with the shift expected for exchange averaging for similar loading levels in a sample of yellow AgA. Considering the uncertain nature and location of the supposedly larger silver clusters there is little to be gained by speculating about the chemical shifts in AgA-670.

The Temperature Dependence of the ^{129}Xe Chemical Shift. We have measured the temperature dependence of the chemical shift for several samples with different loadings pretreated at 380 K. Some representative spectra are shown in Figures 6

(25) Grosse, R.; Burmeister, R.; Boddenberg, B.; Gedeon, A.; Fraissard, J. *J. Phys. Chem.* **1991**, *95*, 2443.
(26) Gedeon, A.; Burmeister, R.; Grosse, R.; Boddenberg, B.; Fraissard, J. *Chem. Phys. Lett.* **1991**, *179*, 191.
(27) Gedeon, A.; Fraissard, J. *Chem. Phys. Lett.* **1994**, *219*, 440.
(28) McCormick, A. V.; Chmelka, B. F. *Mol. Phys.* **1991**, *73*, 603.
(29) Morton, J. R.; Preston, K. F. In *Electronic Magnetic Resonance of the Solid State*; Weil, J., Ed.; Canadian Society for Chemistry: Ottawa, 1987; p 295.

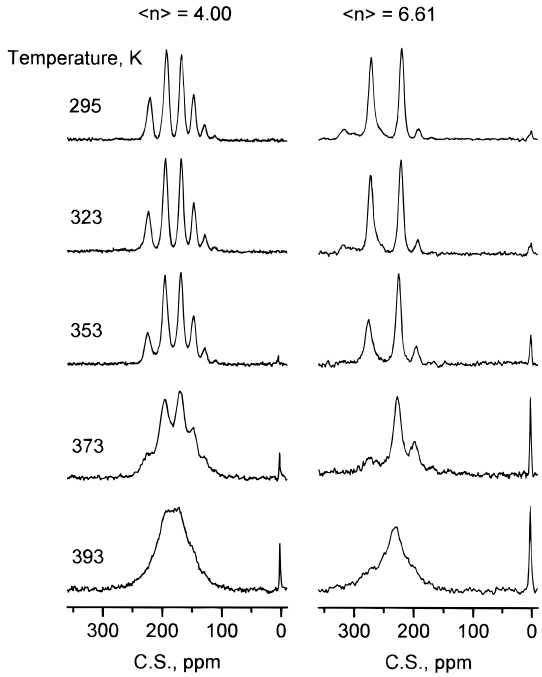

Figure 6. Variable-temperature ^{129}Xe NMR spectra of Xe in AgA-380 for the samples with different loading.

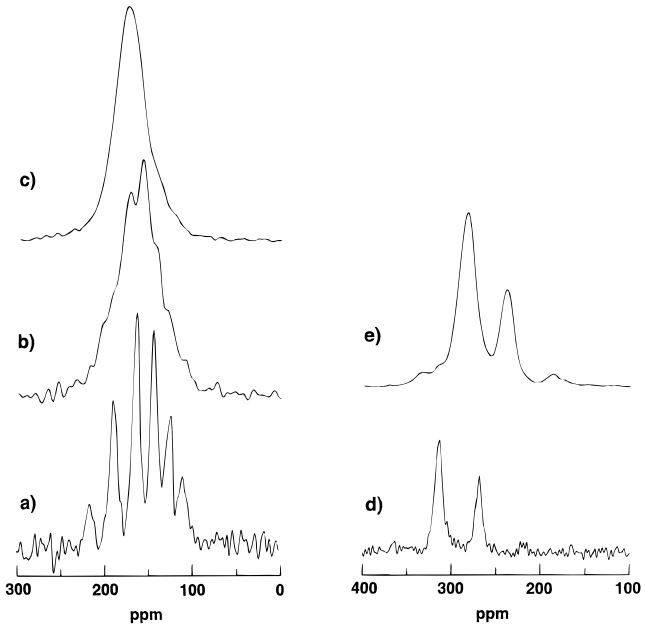

Figure 7. ^{129}Xe spectra of xenon in AgA-380 at low (left) and high (right) Xe loading: sample AgA-380−3.33 at (a) 295 K, (b) 77 K immediately after quenching, and (c) 77 K after 65 h; sample AgA-380−7.55 at (d) 295 K and (e) 77 K after 26 min.

and 7. The chemical shift appears to change linearly down to 145 K for most of the clusters, but the slopes of the lines are all different. With increasing temperature the shifts for Xe_1 and Xe_2 decrease, for Xe_3 the shift is nearly constant, and for higher loadings the shifts all increase. Table 1 gives the slopes and intercepts for the temperature dependencies of the chemical shifts. It is remarkable, that the slopes of most of the lines are very similar to those reported for Xe_n clusters in NaA zeolite. Only for Xe_7 is there a notable difference (since Jameson et al.[10] did not report the experimental errors for NaA, we cannot resolve whether the difference is within the limit of the experimental error).

Above 330 K the lines broaden noticeably, and this effect increases with temperature. At about 390 K the individual lines coalesce, which indicates that xenon motion between the cages has reached the fast exchange limit. The process is completely reversible, and cooling the sample brings back the discrete populations. Several samples were also quenched to liquid nitrogen temperature and in most cases another type of coalescence was observed, as seen for the lower Xe loading in Figure 7 (spectra a−c). The coalescence is largely a result of a substantial increase in line widths, but a slight convergence of the shifts is also expected. Furthermore, there is also evidence of some redistribution of Xe, in that immediately after quenching to 77 K the center of the intensity distribution of the coalesced spectrum, Figure 7b, is still close to that of the room temperature spectrum, but after 65 h at 77 K the center has shifted noticeably downfield, Figure 7c. (Incidentally, we have observed similar coalescence behavior in the spectra of Xe in NaA at 77 K.) At high Xe loadings the broadened lines were still resolved at 77 K but were significantly shifted to higher field, Figure 7 (spectra d,e). The shifting is a continuation of the observed trend with decreasing temperature, but is somewhat greater than expected from the linear extrapolation.

Cross-Polarization Experiments. Cross-polarization ^{129}Xe−^{1}H spectra of adsorbed xenon can be obtained for AgA-380 and AgA-410 samples, although the cross-polarization efficiency is not very high. The ^{129}Xe CP spectra are almost identical to those acquired in single pulse mode (Figure 4, bottom). The observation of CP signals indicates that there is a substantial dipole−dipole interaction remaining between adsorbed xenon and the protons of residual water. Application of high-power proton decoupling does not produce appreciable narrowing of the ^{129}Xe spectra, which indicates, that the line width arises mainly from interactions other than Xe−H dipole−dipole coupling, e.g. inhomogeneous broadening. Magic angle spinning (MAS) indeed produces substantial narrowing of the lines (Figure 4), which is in favor of the latter suggestion.

For some of the samples we also measured the ^{129}Xe−^{1}H cross-relaxation time $T_{CP\ Xe-H}$ and the ^{1}H relaxation time in the rotating frame, $T_{1\rho}$. Table 2 summarizes the data. Within the limits of experimental error, $T_{1\rho}$ does not change with the number of xenon atoms in the α-cage, which indicates that either all the xenon atoms interact with all the protons indiscriminately or all protons in the zeolite are equivalent on the time scale of $T_{1\rho}$. $T_{CP\ Xe-H}$ decreases with increasing cluster size for low n and becomes nearly constant for n between 4 and 7. To a first approximation T_{CPXeH} can be considered to reflect the ^{1}H−^{129}Xe dipole−dipole interaction,[30] and thus the observed decrease in T_{CPXeH} is due to a decrease in the average internuclear distance between xenon and protons. This suggests that at low loading xenon on average prefers to occupy positions inside the cage more distant from water molecules. Jameson et al. in their modeling calculations have assumed that the water molecules are closely associated with the silver atoms located in the 8-ring windows between α-cages,[22] which restricts the passage of Xe.

Spin−Lattice Relaxation Times of Xenon in AgA Zeolite. For a given sample the spin−lattice relaxation time T_1 is the same for all Xe_n peaks, i.e., within the limit of experimental error it is independent of n. The observed T_1, however, depends linearly on the average number $\langle n \rangle$ of xenon atoms in the α-cage (Figure 8). This is to be expected if T_1 is a function of n and the exchange between zeolite cages is sufficiently fast to average the relaxation times. Similar behavior was reported for xenon

(30) Mehring, M. *High-Resolution NMR Spectroscopy in Solids*, 2nd ed.; Spriner: New York, 1980.

Table 1. Dependence of the Chemical Shifts of Xe_n Clusters in AgA on Temperature,[a] $\delta(T) = a + b^* T$

	Xe_1	Xe_2	Xe_3	Xe_4	Xe_5	Xe_6	Xe_7	Xe_8
a (error)	118.8(1.2)	135.4(1.2)	148.2(1.3)	160.3(1.3)	174.3(1.06)	192.67(1.42)	246.07(2.7)	282.16(4.81)
b (error)	−0.0256(0.0044)	−0.022(0.0046)	−0.006(0.005)	0.021(0.005)	0.059(0.004)	0.091(0.005)	0.082(0.0088)	0.118(0.017)
R	−0.77659	−0.71989	−0.25041	0.6677	0.9401	0.9554	0.957	0.949
SD	1.3742	1.44095	1.52327	1.51374	1.437	1.913	1.606	2.42
N	24	24	24	25	33	31	10	7

[a] Parameters: *a*, intercept value and its standard error; *b*, slope value and its standard error; *R*, correlation coefficient; SD, standard deviation of the fit; and *N*, number of data points.

Table 2. $T_{1\rho}$ and $T_{CP\ Xe-H}$ for Sample AgA-380−4.0

parameter	Xe_6	Xe_5	Xe_4	Xe_3	Xe_2
I_0 (arbitrary units)	8.63 ± 1.40	22.43 ± 4.31	21.59 ± 5.21	10.01 ± 2.69	3.33 ± 1.19
$T_{CP\ Xe-H}$, ms	5.74 ± 0.31	5.35 ± 0.36	5.80 ± 0.49	6.65 ± 0.64	8.80 ± 0.94
$T_{1\rho}$, ms	118.63 ± 17.25	113.43 ± 19.34	111.55 ± 23.88	107.7 ± 25.86	135.97 ± 44.65

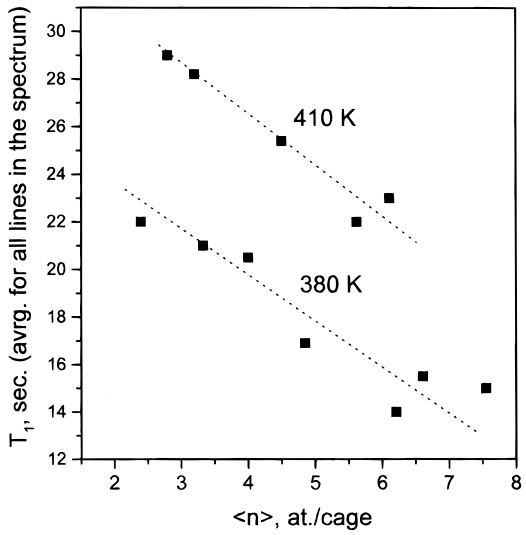

Figure 8. T_1 of Xe in AgA-380 (bottom line) and AgA-410 samples as a function of average loading $\langle n \rangle$.

in NaA,[13] where T_1's of the same order of magnitude were observed. There is also a relationship between T_1 and the temperature of the vacuum treatment of the zeolite. The increase in preparation temperature from 380 to 410 K increases the T_1's at all xenon loadings by about 8 s. As we have already seen from cross-polarization experiments, there is a substantial dipole−dipole interaction between atoms of xenon and protons of the zeolite. Xenon−xenon dipole interactions do not contribute significantly to the observed T_1, since a change of isotopic composition to 79.6% ^{129}Xe does not produce any noticeable effect on the relaxation. Thus, it is reasonable to assume that the main mechanism for relaxation is the dipole−dipole interaction between xenon atoms and protons. For a general case of dipole−dipole relaxation between two unlike nuclei the T_1 can be expressed as follows:[31]

$$\frac{1}{T_1} = \frac{1}{15}\gamma_{Xe}^2\gamma_H^2\hbar^2 I_{Xe}(I_{Xe}+1)\sum_{Xe} r_{Xe-H}^{-6}\left(\frac{6}{1+\omega_{Xe}^2\tau^2} + \frac{2}{1+(\omega_H-\omega_{Xe})^2\tau^2} + \frac{12}{1+(\omega_H+\omega_{Xe})^2\tau^2}\right)\tau \quad (1)$$

Accordingly, the observed difference in spin−lattice relaxation times for the samples prepared at different temperatures can be understood as a result of (a) a decrease in the number of protons or (b) an increase in the average Xe−H distance, at the higher temperature of preparation. Similarly, the decrease in T_1 as the number n of Xe in the cluster increases must arise from a decrease in the average Xe−H distance.

There is also a field dependence of the relaxation time (the number of experimental points, though, is quite limited), with the relaxation faster at lower magnetic field. Thus, for the sample with $\langle n \rangle = 2.4$ atoms/α-cage the figures are $T_1 = 22.0 \pm 1.5$ s at 7 T and $T_1 = 15 \pm 1.7$ s at 4.7 T, and for the sample with $\langle n \rangle = 6.61$ atoms/α-cage $T_1 = 15.5 \pm 1.5$ s at 7 T and $T_1 = 11.3 \pm 1.2$ s at 4.7 T. This field dependence indicates that the relaxation is on the long τ side of the T_1 minimum. Within a model of dipole−dipole relaxation one can attempt to estimate the correlation time for xenon exchange between the proton sites inside the zeolite cages. From eq 1 the observed ratios of the relaxation times obtained at different magnetic fields give a very reasonable correlation time of between 1×10^{-9} and 2×10^{-9} s.

Distribution of Xenon Atoms in α-Cages. The intensities of the lines in the spectra give the distribution of Xe_n clusters. We should note, that deconvolution of the spectra merely into Lorentzian lines produces rather big residuals. This is not entirely surprising, since such a line shape should be expected only for nonrestricted motion in liquids or gases. A distribution of local cage environments together with some restriction of motion should lead to a deviation of the experimentally observed lines from Lorentzian. We found that utilization of mixed Lorentzian−Gaussian lines considerably reduces the decomposition residuals, with a linear combination of 70% Gaussian and 30% Lorentzian shapes giving the best fit, as used in this work.

If $\langle n \rangle$ is the average number of xenon atoms per cage, as obtained from mass balance, and $I(n)$ is the integral intensity of the component, then the fraction $P(n)$ of the α-cages with n xenon atoms is

$$P(n) = \langle n \rangle \frac{I(n)}{n\sum_1^8 I(n)} \quad (2)$$

The fraction of empty α-cages is obtained from the balance, since $\sum_0^8 P(n) = 1$. Experimental data on the population distribution are collected in Table 3. It is interesting to compare these data with some theoretical models for distribution of adsorbed molecules in the cages of zeolites. One such model, which takes into account the finite volumes of the Xe atoms, produces a hypergeometric distribution.[32] For the limiting case

(31) Abragam, A. *The principles of Nuclear Magnetism*; University Press: Oxford, 1961; p 294.

Table 3. Distibution of the Xe_n Clusters in the α-Cages of Zeolite AgA

	n in α-cage								
$\langle n\rangle_{adsorb}$	0	1	2	3	4	5	6	7	8
0.98	0.33	0.4165	0.19012	0.0539	0.00539	0	0	0	0
1.35	0.26	0.3564	0.231525	0.10845	0.036113	0.01215	0	0	0
2.2	0.11	0.198	0.2816	0.233933	0.13805	0.03696	0	0	0
2.2	0.1	0.2266	0.2706	0.223667	0.1254	0.042108	0.006967	0	0
2.4	0.06	0.2376	0.2568	0.22	0.1404	0.06096	0.0204	0	0
2.8	0.04	0.1568	0.231	0.255733	0.2016	0.09576	0.021467	0	0
3.2	0.05	0.112	0.1712	0.209067	0.2232	0.16704	0.065067	0	0
3.33	0.02	0.11655	0.16317	0.22644	0.24309	0.168498	0.06549	0	0
4.0	0.01	0.038	0.092	0.177333	0.292	0.2704	0.114	0.006286	0
4.5	0	0	0.07425	0.132	0.244125	0.3339	0.21825	0	0
4.85	0	0	0.0388	0.085683	0.215825	0.3589	0.274025	0.033257	0
5.62	0	0	0.01967	0.024353	0.060415	0.234916	0.5339	0.126851	0
6.11	0	0	0	0	0.02444	0.130754	0.550918	0.29328	0
6.21	0	0	0	0	0	0.116748	0.603405	0.266143	0.017854
6.61	0	0	0	0	0	0.050236	0.384482	0.470254	0.095019
7.55	0	0	0	0	0	0	0.047817	0.35485	0.597394

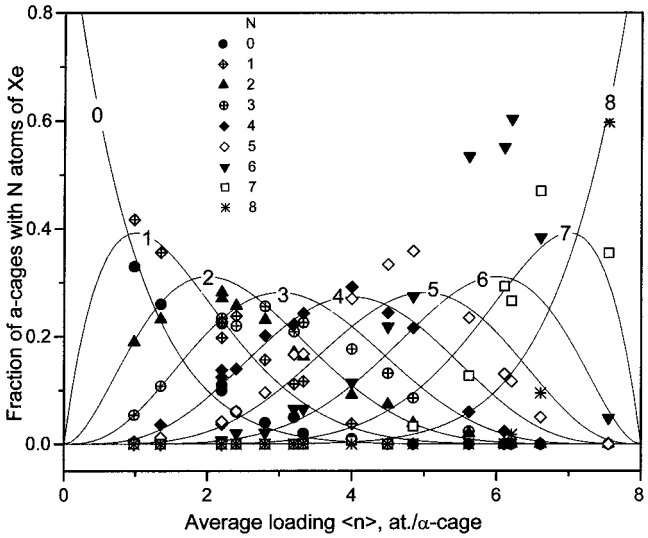

Figure 9. Distribution of the cages with *n* atoms of xenon as a function of $\langle n\rangle$: comparison with hypergeometric distribution (Table 3, distributions of Xe_n clusters in the samples). For (Xe_7' + Xe_7'') and (Xe_8' + Xe_8'') pairs the total intensities of the pairs are used as Xe_7 and Xe_8 intensities, respectively.

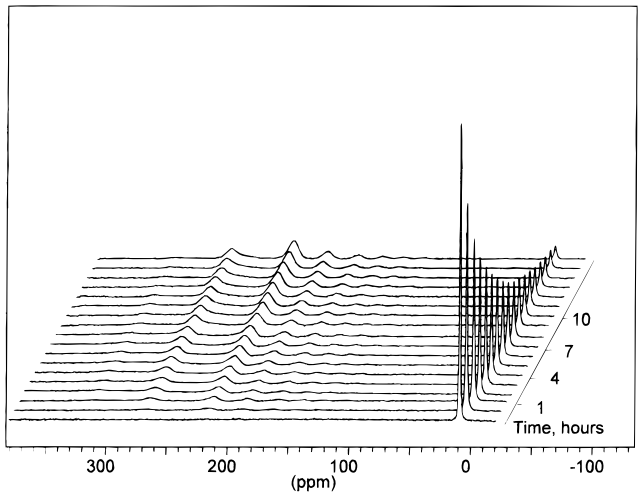

Figure 10. ^{129}Xe NMR spectra, recorded just after loading of the AgA-380 sample, and showing adsorption and redistribution of xenon inside the zeolite.

of a very large number of cages, the distribution can be expressed [10] as

$$H_n(\langle n\rangle) = \frac{\langle n\rangle^n (k - \langle n\rangle)^{(k-n)}}{k^k} \frac{k!}{n!}(k-n)! \qquad (3)$$

where H_n is the fraction of α-cages containing *n* xenon atoms and *k* is the maximum number of atoms that can fit into a cage. The applicability of this distribution was discussed extensively in connection with the Xe_n populations in NaA,[8−10] and recently, AgA.[22] Figure 9 shows our data for the Xe_n populations in AgA in comparison with the hypergeometric distribution. Since Xe_8 is the largest cluster observed experimentally, we can assume, that the maximum number of sites in the AgA α-cage *k* is eight (i.e. the same as in the case of NaA[10]). As one can see from Figure 9, the hypergeometric distribution describes the observed populations reasonably well only for mean Xe loadings below 4. The experimental distribution at higher loadings is noticeably sharper than hypergeometric and shifted toward the lower occupancies. The nature of these deviations was the subject of comprehensive experimental and theoretical studies,[8−10,16,17,28] and was successfully reproduced by grand canonical Monte Carlo simulations.[8−10,13] We note that our distributions for AgA agree very well with the calculations reported recently by Jameson et al.[22]

Diffusion of Xe into the Crystallites of Zeolite AgA-380. The slow adsorption and redistribution of Xe in the crystallites of AgA makes it possible to observe these processes directly by NMR (Figure 10). The changing pressure in the sample tube can be monitored directly through the chemical shift of the gaseous Xe, which depends on the density as $\delta(\rho) = 0.548\rho + (1.69 \times 10^{-4})\rho^2$ [33] (ρ is the gas density in amagat). Therefore, the time dependence of the chemical shift gives the kinetics of the xenon adsorption. The observed kinetics can be fitted by a single-exponential decay, giving the constant for xenon diffusion into the crystallite. This constant depends on the temperature of the vacuum pretreatment and, therefore, the residual water content, and for five of the samples studied was between 1×10^{-5} and 3×10^{-5} s^{-1}. The uptake does not seem to vary a great deal with pressure, which must change as the xenon is adsorbed from the constant volume of the sealed tube. It is also interesting to note that xenon atoms "pile up" in the outermost shell of the zeolite particles with cage occupancies far higher than those achieved at equilibrium. As remarked earlier, the equilibrium distributions are not reached until a long

(32) Guemez, J.; Velasco, S. *Am. J. Phys*. **1987**, *55*, 154.

(33) Jameson, C. J.; Jameson, A. K.; Cohen, S. M. *J. Chem. Phys*. **1973**, *59*, 4540.

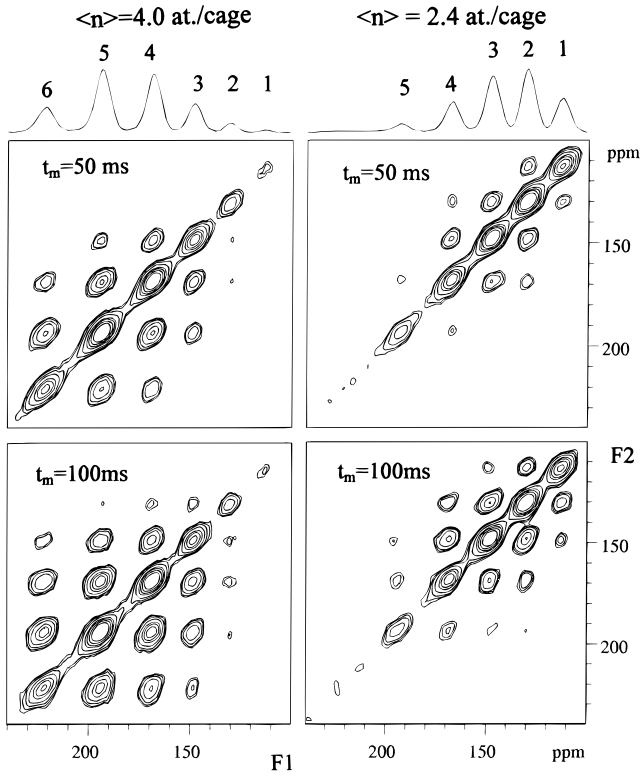

Figure 11. 2D EXSY spectra of two samples with different loadings registered with different mixing times.

time after the xenon has been completely adsorbed. This can be understood more clearly once the kinetic results from the 2D-EXSY experiments are considered.

Determination of Kinetic Parameters from 2D-EXSY Spectra. The 2D-EXSY technique, originally introduced by Jeener,[34] has found broad applications for the study of chemical exchange in liquids. The presence of chemical exchange within a time of the order of the mixing time (t_{mix} in the pulse sequence) gives rise to off-diagonal cross-peaks in the 2D spectrum between the resonances of the sites involved in the exchange. Some applications of the technique to zeolite chemistry have been reported recently,[17,35−37] including a study of Xe in NaA which is of particular relevance to the current work.[17]

Figure 11 shows typical 2D-EXSY NMR spectra of Xe in AgA obtained with various mixing times for samples of different average loadings. The spectra reveal well-resolved cross-peaks between the signals from different xenon clusters that unambiguously confirm exchange of xenon atoms between adjacent α-cages. The cross-peaks provide information about the exchange pathways, and their integrated intensities are related to the rates of exchange. The coupled differential equations that describe the magnetization m along the z-axis during the experiment can be written in the form

$$\dot{m} = \mathbf{R}m \tag{4}$$

where **R**, for the case without cross-relaxation, is a sum of the kinetic and relaxation matrixes:[23]

$$\mathbf{R} = \begin{pmatrix} -\frac{1}{T_{11}} - K_{12} - \ldots - K_{1n} & K_{12} \ldots & K_{1n} \\ K_{21} & -\frac{1}{T_{12}} - K_{21} - \ldots - K_{2n} \ldots & K_{2n} \\ \ldots & \ldots\ldots & \ldots \\ K_{n1} & K_{n2} \ldots & -\frac{1}{T_{1n}} - K_{n1} - \ldots - K_{nn} \end{pmatrix} \tag{5}$$

Rates of exchange can be obtained by solving the magnetization transfer matrix simultaneously for all sites. Formal solution of eq 4 at $t = t_m$ (t_m = mixing time) is given by eq 6

$$\mathbf{M}(t_m) = e^{-\mathbf{R}t_m} M(0) \tag{6}$$

where $\mathbf{M}(0)$ is a column matrix of equilibrium magnetization of each site. The most efficient approach to solving this system is by the application of matrix methods,[23,24,38] and the matrix **R** is given by

$$\mathbf{R} = -\frac{\ln \mathbf{A}}{t_m} = -\frac{\mathbf{X}(\ln \Lambda)\mathbf{X}^{-1}}{t_m} \tag{7}$$

where $\mathbf{A}_{ij} = \mathbf{I}_{ij}(t_m)/\mathbf{M}_j(0)$ is the experimental matrix of normalized intensities, X is the square matrix of eigenvectors of **A**, such that $\mathbf{X}^{-1}\mathbf{A}\mathbf{X} = \mathbf{L} = \mathrm{diag}(\mathrm{l}_i)$ and l_i are the eigenvalues of **A**. Numerical solution of eq 7 gives a complete set of the rate constants for the system in exchange.[24]

Since the xenon resonances are sensitive to the xenon cage occupancy, the transport of a single xenon atom not only alters the resonance frequency of the xenon atoms in the cage it has left but also changes the resonance of the xenon atoms in the cage it moves to. Thus, transfer of a single xenon atom changes the magnetizations simultaneously in two cages. Because of this, in the systems with discrete populations of xenon, the matrix elements of the magnetization exchange matrix are not equal to those of the xenon exchange matrix. The discreteness of the cage populations must be taken into account, and for a complete analysis all transfer mechanisms and the corresponding rates must be considered. The magnetization rate constants K_{mn}, obtained from the analysis of the experimental magnetization transfer matrix, describe the pseudo-first-order exchange rate from site n to site m. These rate constants are a composite of several microscopic rate constants, and, following,[13] can be expressed as:

$$K_{mn} = k_{mn}\, \mathrm{f}(m-1) \qquad \text{when } |n-m| > 1 \tag{8a}$$

$$K_{m,m-1} = k_{m,m-1}\, \mathrm{f}(m-1) + \sum_i^8 i k_{mi}\, \mathrm{f}(i) \tag{8b}$$

$$K_{m,m+1} = k_{m,m+1}\, \mathrm{f}(m-1) + m\sum_i^8 k_{i,m+1}\, \mathrm{f}(i-1) \tag{8c}$$

There are constraints on the K_{mn} and the k_{mn} values from principles of detailed balance:

$$K_{mn} n\, \mathrm{f}(n) = K_{nm} m\, \mathrm{f}(m)$$

$$k_{mn}/k_{nm} = m\, \mathrm{f}(m)\, \mathrm{f}(n-1)/n\, \mathrm{f}(n)\, \mathrm{f}(m-1)$$

Thus, only the upper triangle of the rate constant matrix needs

(34) Jeener, J.; Meier, B. H.; Bachmann, P.; Ernst, R. R. *J. Chem. Phys.* **1979**, *71*, 4546.
(35) Kritzenberger, J.; Gaede, H. C.; Shore, J. S.; Pines, A.; Bell, A. *J. Phys. Chem.* **1994**, *98*, 10173.
(36) Moudrakovski, I.; Ratcliffe, C.; Ripmeester, J. *Appl. Magn. Reson.* **1996**, *10*, 559.
(37) Moudrakovski, I.; Ratcliffe, C.; Ripmeester, J. *Appl. Magn. Reson.* **1995**, *8*, 385.
(38) Perrin, C.; Gipe, R. K. *J. Am. Chem. Soc.* **1984**, *106*, 4036.

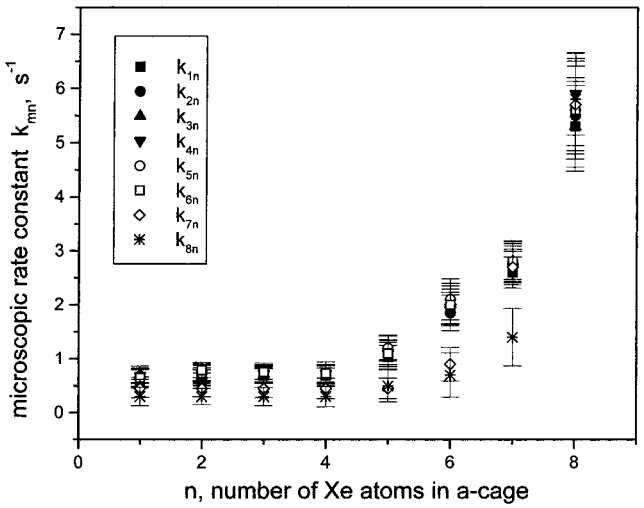

Figure 12. Microscopic rate constants k_{mn} as obtained from 2D EXSY experiments. Here m stands for the number of atoms in the Xe_n cluster which is forming and n is the size of the cluster the atom is leaving: $Xe_n + Xe_{m-1} = Xe_{n-1} + Xe_m$. For (Xe7′, Xe7″) and (Xe8′ and Xe8″) clusters combined intensities of the pairs were used in the calculations of the constants, and for n and m equal to 7 or 8 only the combined constants for two sites together are obtained. Bars around the points represent not error bars but scattering of the k_{mn} around the mean value.

to be found. The rates of exchange can be obtained directly by solving eq 6 together for all sites, taking into account the discreteness of the cage populations.[13,17] We should emphasize that for this system with its multisite exchange the complete set of rate constants could be estimated from a single experiment only by using the 2D-EXSY technique.

The rate constants determined in this way for xenon transfer between the cages of AgA zeolite depend on the number of xenon atoms in the cage, and for the cages with xenon occupancy lower than 6 are of the order of 1 s^{-1} (Figure 12). The increase of the rate constants with occupancy can be explained as a result of decreasing sorption energy with rise of population,[17] and this has been reproduced quantitatively for xenon in NaA by the grand canonical Monte Carlo simulations.[13] In agreement with the results of ref 13, we find that the rate constants are significantly smaller when the number of xenon atoms in the destination cage is six or seven (i.e., it becomes much more difficult for the atom to enter the cage). It is interesting to note that the complete matrix of microscopic rate constants for our samples is quite similar to that reported by Jameson et al. for NaA, except that the values are larger by a factor of 2−2.4. While some increase in the rate constants for the samples prepared at 410 K compared with those treated at 380 K might be anticipated, we did not find any appreciable difference. This, however, could be the result of the limited experimental accuracy of the technique.

A few words must be said concerning the determination of the exchange constants by this method and the accuracy of the technique. Experimental errors in the determination of kinetic parameters with the 2D-EXSY technique are known to be extremely sensitive to the signal-to-noise level.[23,38] For our samples it means that even for the best signal-to-noise we obtained, we cannot expect the error to be less than 30−40%. We also found that the choice of experimental parameters for the 2D-EXSY experiments, particularly the mixing time t_m, can dramatically affect the results. At short mixing times the intensities of the cross signals are small, which makes determination of their integral intensities less reliable. Furthermore, the use of long mixing times, which does produce appreciable

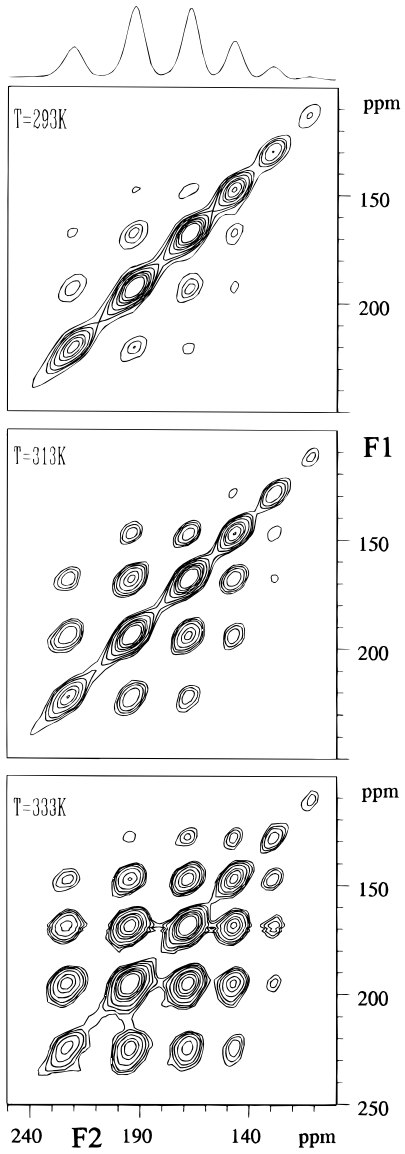

Figure 13. 2D EXSY spectra of AgA-380−4.0, recorded with the same mixing time t_m = 10 ms at three different temperatures. Estimated E_a = 45 ± 10 kJ/mol.

intensities, definitely is not a good solution to the problem, since multistep exchange must then be taken into account.

From the variable-temperature 2D exchange experiments (Figure 13), the average activation energy of xenon transfer between the different cages can be estimated as E_a = 45 ± 10 kJ/mol, noticeably lower than the value for NaA zeolite. The higher k_{mn} and lower E_a for the intercage exchange in AgA as compared to NaA indicate that there is a greater obstruction at the intercage window by the sodium cations.

Conclusions

The adsorption and distribution of xenon in AgA zeolite have been studied by applying ^{129}Xe NMR. Exchange of xenon between the α-cages of AgA zeolite treated in a vacuum at 380 or 410 K is slow, and separate lines are observed in the ^{129}Xe NMR spectrum for the cages with different populations of xenon. The cages containing between 1 and 6 xenon atoms exhibit single lines with a separation between the signals of about 20−25 ppm, while for Xe_7 and Xe_8 clusters the separation of the chemical shifts increases and they appear to be present in two different states $Xe_7' + Xe_7''$ and $Xe_8' + Xe_8''$. The

population distribution has been studied for a broad range of loadings, and it appears that it cannot be described in terms of a simple hypergeometric distribution. Only a single broad line is observed for xenon in "orange" AgA zeolite treated at 670 K, indicating that there is relatively easy exchange between the cages of this material.

The NMR lines for Xe_n clusters in the α-cages of AgA are all almost equally shifted to low field relative to the clusters in NaA zeolite. This is opposite to the high-field shift observed for xenon in silver-exchanged X and Y zeolites[25−27] and leads one to conclude that Xe is not in contact with the special type of Ag^+ ion postulated to be the origin of the shift in AgX and AgY. Packing considerations suggest that Xe_8 clusters could not occur if any of the postulated silver clusters were present inside the α-cages. The silver clusters must therefore be in the β-cages. Calculations[22] suggest that the packing of more than 2 water molecules into each α-cage would increase the shift but would reduce the occurrence of Xe_8 and significantly alter the shift increments observed when the Xe cluster size increases. An interaction of Xe with a silver cluster, presumably through a 6-ring window, therefore still seems a likely source for the 40 ppm difference between xenon chemical shift in NaA and AgA zeolites, though the suggested[22] Fermi contact interaction seems unlikely on the grounds that EPR signals cannot be found. This problem remains unresolved. Aside from the 40 ppm difference, the increasing chemical shifts for Xe_n clusters and their distribution in the cages of AgA treated at low temperature show very similar behavior to that observed for NaA and explained by grand canonical Monte Carlo simulations.[8−10,13] For AgA zeolite treated in a vacuum at 670 K and not containing residual water, the ^{129}Xe chemical shift for concentrations below 1 atom/cage is almost independent of loading and close to that of Xe_1 in NaA, again suggesting restricted accessibility for the charged silver clusters to xenon and their location inside the sodalite cages.

The dynamics of xenon exchange between the cages have been studied by 2D-EXSY NMR. All the rate constants can be directly obtained from the analysis of the 2D-NMR data, and are found to be of the order of 1 s^{-1} for the cages with occupancy lower than 6 atom/cage. The constants increase with the cage occupancy, showing the same trends as seen previously for xenon in NaA.[13] From variable-temperature 2D-EXSY experiments the activation energy of xenon transfer between the different cages can be estimated as $E_a = 45 \pm 10$ kJ/mol, significantly lower than that in NaA zeolite. This is likely a result of a larger effective opening of the intercage window in AgA.

Acknowledgment. The authors thank Mr. J. T. Bennett for expert technical assistance.

Supporting Information Available: Graph of ^{129}Xe chemical shifts of xenon in AgA-380 zeolite vs temperature (1 page, print/PDF). See any current masthead page for ordering information and Web access instructions.

JA973748Z